NeuroImage 81 (2013) 283–293

Contents lists available at SciVerse ScienceDirect

NeuroImage

journal homepage: www.elsevier.com/locate/ynimg

A novel approach to predict subjective pain perception from single-trial laser-evoked potentials

G. Huang [a,1], P. Xiao [b,1], Y.S. Hung [a], G.D. Iannetti [c], Z.G. Zhang [a,*], L. Hu [b,**]

[a] Department of Electrical and Electronic Engineering, The University of Hong Kong, Hong Kong, China
[b] Key Laboratory of Cognition and Personality (Ministry of Education) and School of Psychology, Southwest University, Chongqing, China
[c] Department of Neuroscience, Physiology and Pharmacology, University College London, UK

ARTICLE INFO

Article history:
Accepted 9 May 2013
Available online 16 May 2013

Keywords:
Pain
Laser-evoked potentials (LEPs)
Pain prediction
Classification
Regression

ABSTRACT

Pain is a subjective first-person experience, and self-report is the gold standard for pain assessment in clinical practice. However, self-report of pain is not available in some vulnerable populations (e.g., patients with disorders of consciousness), which leads to an inadequate or suboptimal treatment of pain. Therefore, the availability of a physiology-based and objective assessment of pain that complements the self-report would be of great importance in various applications. Here, we aimed to develop a novel and practice-oriented approach to predict pain perception from single-trial laser-evoked potentials (LEPs). We applied a novel single-trial analysis approach that combined common spatial pattern and multiple linear regression to automatically and reliably estimate single-trial LEP features. Further, we adopted a Naïve Bayes classifier to discretely predict low and high pain and a multiple linear prediction model to continuously predict the intensity of pain perception from single-trial LEP features, at both within- and cross-individual levels. Our results showed that the proposed approach provided a binary prediction of pain (classification of low pain and high pain) with an accuracy of 86.3 ± 8.4% (within-individual) and 80.3 ± 8.5% (cross-individual), and a continuous prediction of pain (regression on a continuous scale from 0 to 10) with a mean absolute error of 1.031 ± 0.136 (within-individual) and 1.821 ± 0.202 (cross-individual). Thus, the proposed approach may help establish a fast and reliable tool for automated prediction of pain, which could be potentially adopted in various basic and clinical applications.

© 2013 Elsevier Inc. All rights reserved.

Introduction

Pain is an unpleasant multidimensional experience associated with real or potential tissue damage (Loeser and Treede, 2008). Therefore, pain experience does not simply reflect sensory information but can be substantially influenced by various psycho-social contexts (e.g., the gender of experimenter) (Aslaksen et al., 2007) and psycho-physiological factors (e.g., fluctuations in vigilance and attention). Since pain is a subjective first-person experience, self-report (e.g., Visual Analog Scales [VAS] and Numeric Rating Scales) is the gold standard for the determination of the presence, absence, and intensity of pain perception in clinical practice (Cruccu et al., 2010; Haanpaa et al., 2010). While self-report of pain provides important clinical information for the adequate treatment of pain patients in most situations (Brown et al., 2011), it fails to be used in some vulnerable populations (e.g., patients with disorders of consciousness, including coma, vegetative state, and minimally conscious state) (Schnakers and Zasler, 2007). Lack or any inaccuracy of pain assessment can lead to inadequate or suboptimal treatment of pain in these vulnerable patients, which may lead to various additional clinical problems (e.g., psychological distress or depression, the development of chronic pain) (Roulin and Ramelet, 2012; Zwakhalen et al., 2006). Although reliable pain assessment is important to adequately treat patients suffering from persistent pain (Gagliese and Melzack, 1997; Zwakhalen et al., 2006), it is extremely difficult to detect and monitor pain in specific clinical populations, such as non-communicative patients with disorders of consciousness (Schnakers et al., 2010). In addition, the brain damage of these patients may lead to confused, stereotyped, and uncoordinated behaviors (Roulin and Ramelet, 2012; Schnakers and Zasler, 2007), which is the barrier to adopt behavioral responses as pain indicators. Therefore, the availability of a physiology-based and objective assessment of pain that complements the self-report of pain would be of great importance in basic and clinical applications.

Nowadays, electroencephalographic (EEG) responses elicited by nociceptive laser heat pulses that selectively excite nociceptive free nerve endings in the epidermis (Bromm and Treede, 1984) are widely adopted to investigate the peripheral and central processing of nociceptive sensory input (Iannetti et al., 2003; Treede et al., 2003). Such laser-evoked potentials (LEPs) are mediated by the activation of type-II Aδ mechano-heat nociceptors (Treede et al., 1995) and spinothalamic neurons in the anterolateral quadrant of the spinal cord (Treede et al., 2003). LEPs consist of several transient responses that are time locked and phase locked to the onset of laser stimuli. The largest LEP response consists of a biphasic negative–positive complex (N2 and P2 waves),

* Corresponding author. Fax: +852 25598738.
** Corresponding author. Fax: +86 23 68252983.
E-mail addresses: zgzhang@eee.hku.hk (Z.G. Zhang), huli@swu.edu.cn (L. Hu).
[1] These authors contributed equally.

1053-8119/$ – see front matter © 2013 Elsevier Inc. All rights reserved.
http://dx.doi.org/10.1016/j.neuroimage.2013.05.017

maximal at the scalp vertex (Bromm and Treede, 1984) and largely reflecting the activity of the bilateral operculoinsular and anterior cingulate cortex (Garcia-Larrea et al., 2003). The strong relationship between the N2 and P2 amplitudes in LEPs and the intensity of pain perception have been well characterized (Bromm and Treede, 1991; Garcia-Larrea et al., 1997; Iannetti et al., 2005; Kakigi et al., 1989), and the correlations between N2 and P2 latencies and the intensity of pain perception were also reported (Iannetti et al., 2005). All these findings inspire us to explore the possibility of objective assessment of pain based on the single-trial LEP features related to latencies and amplitudes of N2 and P2 waves.

The aim of the present study was to develop a novel approach to rapidly and reliably predict pain from single-trial LEP features (Fig. 1), which can be achieved through the following two major steps. First, a novel method that combines common spatial pattern (CSP) and multiple linear regression (MLR) was proposed to achieve an automated and reliable single-trial estimate of LEP features. Second, a Naïve Bayes classifier and a multiple linear prediction model were trained to respectively distinguish low and high pain and predict the intensity level of pain perception from single-trial LEP features. Such training and predicting were achieved at both within-individual level, where the classifier and prediction model were trained on and applied to single-trial LEPs from the same individual, and cross-individual level, where the classifier and prediction model were trained on a cohort of individuals and applied to another individual.

Materials and methods

Experimental design and EEG recording

Twenty-nine healthy participants (9 females and 20 males) aged 17–25 years (mean 22.2 ± 1.9), without a history of chronic pain, participated in the study. All participants gave written informed consent, and the local ethics committee approved the experimental procedures.

Radiant-heat stimuli were generated by an infrared neodymium yttrium aluminum perovskite (Nd:YAP) laser with a wavelength of 1.34 μm (Electronical Engineering, Italy). Laser pulses activate directly nociceptive terminals in the most superficial skin layers (Baumgartner et al., 2005; Iannetti et al., 2006). Laser pulses were directed at the dorsum of left hand on a squared area (5 × 5 cm) defined prior to the beginning of the experimental session. A He–Ne laser pointed to the area to be stimulated. The laser pulse was transmitted via an optic fiber and its diameter was set at approximately 7 mm (~38 mm^2) by focusing lenses. The pulse duration was 4 ms, and four different energies (E1: 2.5 J; E2: 3 J; E3: 3.5 J; E4: 4 J) of stimulation were used. After each stimulus, the laser beam target was shifted by approximately 1 cm in a random direction to avoid nociceptor fatigue or sensitization.

Prior to data collection, a small number of laser pulses with different stimulus energies were imposed on the stimulated territory to ensure that the participants were familiar with the stimulation. Ten laser pulses at each of the four stimulus energies (E1–E4) were delivered, in random order, for a total of 40 pulses per participant (Fig. 2, top panel). The inter-stimulus interval (ISI) was ranged between 10 and 15 s. An auditory tone was delivered 3–6 s after the presentation of each laser pulse to remind the participants to rate the intensity of the painful sensation elicited by the laser stimulus, using a VAS ranging from 0 (not pain) to 10 (pain as bad as it could be).

Participants were seated in a comfortable chair in a silent, temperature-controlled room. They wore protective goggles and were asked to focus their attention on the stimuli and relax their muscles. The EEG data were recorded using a 64-channel Brain Products system (Brain Products GmbH, Munich, Germany; pass band: 0.01–100 Hz; sampling rate: 1000 Hz) using a standard EEG cap based on the extended 10–20 system. The nose was used as the reference channel, and all channel impedances were kept lower than 10 kΩ. To monitor ocular movements and eye blinks, electro-oculographic signals were

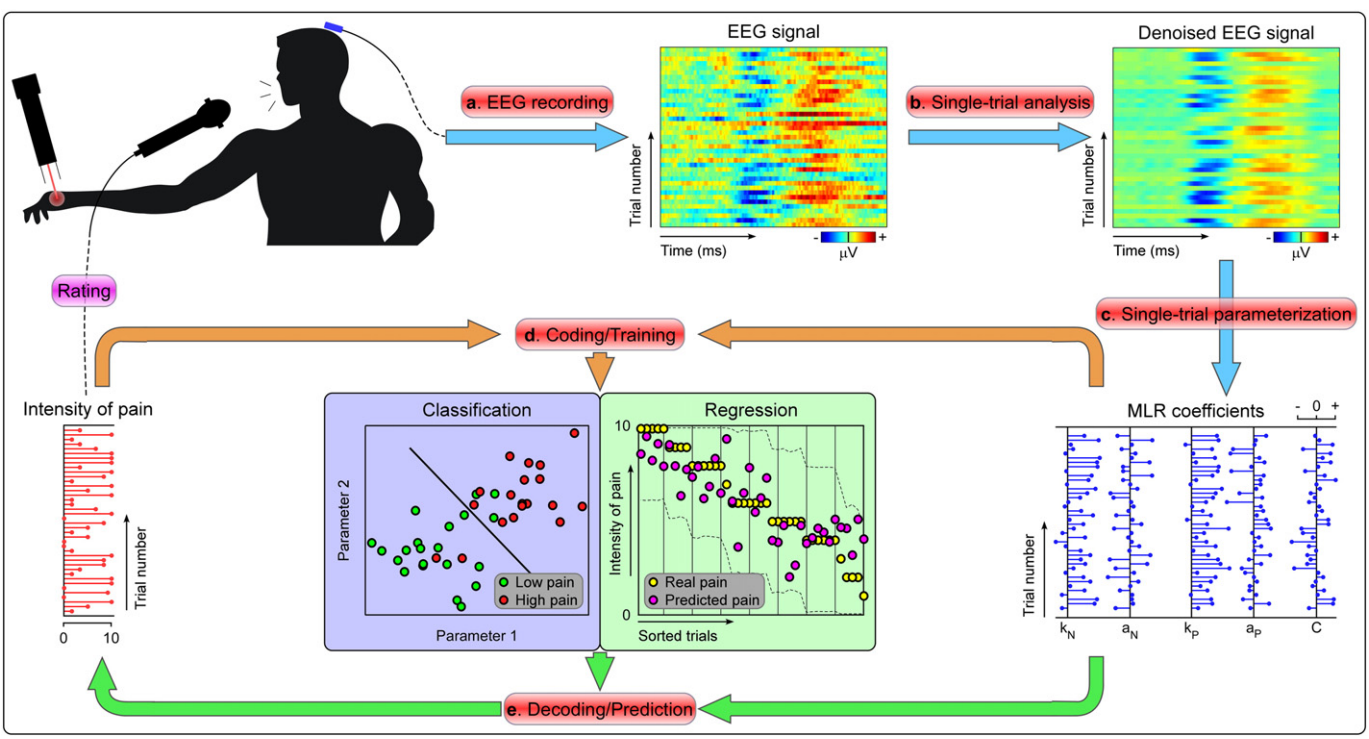

Fig. 1. EEG based pain prediction. EEG signal is recorded (a) following the nociceptive stimulation on the target territory of human body, and the subject rates verbally the intensity of pain perception after each nociceptive stimulus. Noise contaminated in the recorded EEG signal is removed using effective single-trial analysis techniques (e.g., ICA, CSP) (b). The denoised EEG signal is further parameterized using MLR (c), and a set of MLR coefficients, which capture single-trial variability of LEP responses (e.g., N2 and P2 latency and amplitude), are obtained. The relationship between MLR coefficients and intensity of pain perception on a single-trial basis can be coded/trained (d) using both classification and regression approaches. Based on the models, the intensity of pain perception can be decoded/predicted (e) using estimated single-trial MLR coefficients.

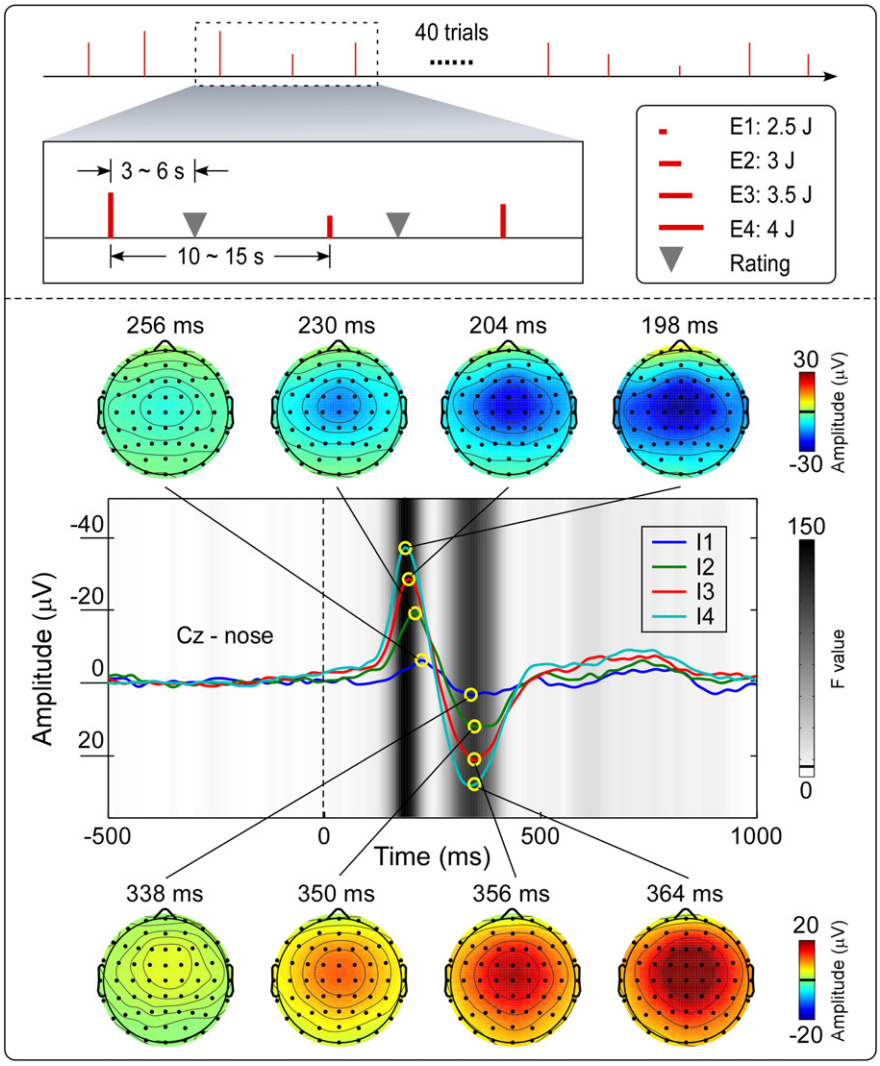

Fig. 2. Experiment design and laser-evoked brain potentials. Top panel: Laser-evoked brain responses were recorded following the laser stimulation of the left hand dorsum. Four different stimulation energies (E1: 2.5 J; E2: 3 J; E3: 3.5 J; E4: 4 J) were used, and 10 trials of each of the 4 stimulation energies were delivered in random order, for a total of 40 trials. The inter-stimulus interval was randomly distributed between 10 and 15 s. Between 3 and 6 s after each laser stimulus, subjects were reminded by an acoustical signal (beep) to rate verbally the intensity of pain perception using a VAS ranging from 0 to 10. Bottom panel: Group averages and scalp topographies of LEPs at different intensity of pain perception (I1–I4). Group-level average LEPs were recorded at electrode Cz (nose reference), and categorized according to the intensity of pain perception (colored waveforms). Gray scale represents the F-values obtained for each time point using a one-way repeated measures ANOVA to assess the effect of "intensity of pain perception" on LEPs. Both N2 and P2 amplitudes showed the strongest modulation with the "intensity of pain perception" (marked in dark gray).

simultaneously recorded from 4 surface electrodes: one pair placed over the upper and lower eyelids, and the other pair placed 1 cm lateral to the outer corner of the left and right orbits.

Data analysis: single trial feature extraction

Since the magnitude of laser-evoked brain responses is often several factors smaller than the magnitude of background EEG and non-cortical artifacts (Hu et al., 2010), the prediction of pain perception from single-trial LEPs would rely on advanced signal processing techniques to (1) enhance greatly the signal-to-noise ratio (SNR) and (2) estimate automatically and reliably single-trial LEP features. Thus, we proposed to enhance the SNR of single-trial LEPs using the combination of (1) bandpass filtering (BPF), (2) independent component analysis (ICA), and (3) common spatial pattern (CSP), and to estimate single-trial LEP features using (4) multiple linear regression (MLR) (Fig. 3, top panel). BPF and ICA were applied to perform a filter on EEG recordings in the spectral and spatial domains respectively, to remove irrelevant noise and artifacts. CSP was adopted to further enhance the SNR of LEP responses by retrieving stimulus-evoked EEG responses from spontaneous EEG activity. Finally, MLR was used to automatically parameterize single-trial LEP responses using MLR coefficients, which captured the variability of single-trial N2 and P2 latency and amplitude. The four analytic steps were detailed in the following subsections.

Bandpass filtering and independent component analysis

To provide a filter in the spectral domain, continuous EEG data were bandpass filtered between 1 and 30 Hz (zero-phase digital filtering) (Delorme and Makeig, 2004). EEG trials were extracted using an analysis window of 1500 ms (500 ms pre-stimulus and 1000 ms post-stimulus), and baseline corrected using the pre-stimulus time interval.

Following, EEG trials contaminated by eye-blinks and movements were corrected using the ICA algorithm (Delorme and Makeig, 2004; Jung et al., 2001; Makeig et al., 1997). As described by Mognon et al. (2011), artifacts related to eye-blinks and movements could be automatically identified based on the combination of stereotyped artifact-specific spatial and temporal features. In all datasets, the independent components having a large EOG channel contribution and a frontal

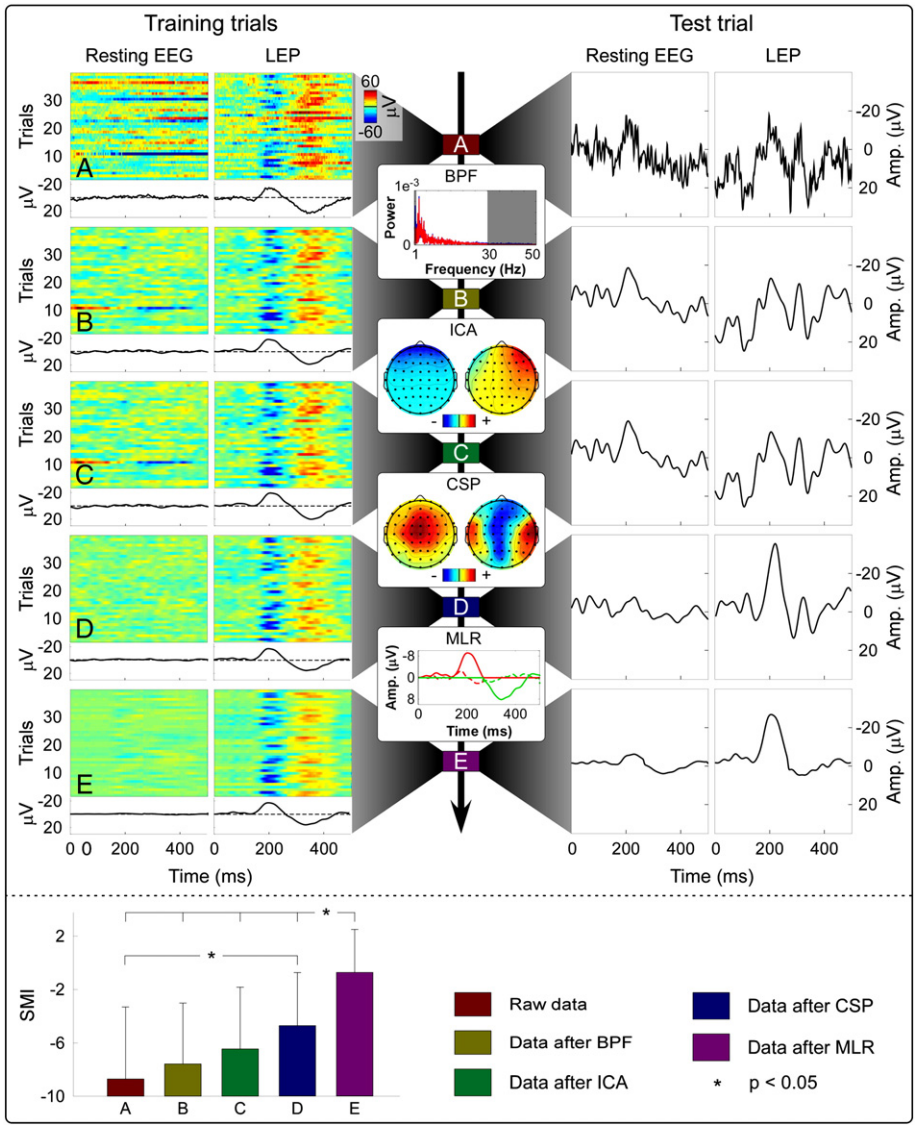

Fig. 3. Flowchart describing the procedure to enhance the SNR of single-trial LEP responses. Top panel: The EEG responses (A, both resting EEG and LEP responses, and for both training and test), measured at Cz, were bandpass filtered between 1 and 30 Hz (step 1). In the training dataset, noise trials in the filtered EEG responses (B) were corrected using ICA (step 2), and the ICA corrected EEG responses (C) were spatially filtered using CSP (step 3). The spatially-filtered EEG responses (D) were further modeled using MLR (step 4). This procedure generated both single-trial EEG responses with enhanced SNR (E) and the corresponding filter models (ICA, CSP, and MLR models), which were applied on the test trial to significantly enhance its SNR (from top to bottom). Bottom panel: SMI, indicated the ratio between "LEP-like" responses (signal) and "LEP-irrelevant" residual (noise), was used to assess the filter effect of each single-trial analysis step. One-way repeated-measures ANOVA revealed that the single-trial analysis steps can significantly enhance the SMI ($F = 79.24$, $p < 0.001$).

scalp distribution were removed, and the remaining independent components were used to reconstruct the denoised EEG trials.

Common spatial pattern

CSP is a mathematical tool to decompose two populations of multivariate signals into a set of spatial patterns, which maximize their differences in terms of variance (Muller-Gerking et al., 1999; Ramoser et al., 2000). This method was first applied in the field of EEG analysis to detect abnormalities (Koles, 1991; Koles et al., 1990), and has recently been shown to be a powerful technique in brain–computer interface research for discriminating different mental intentions (Blankertz et al., 2008). In the present study, one population consisted of EEG recordings before the presentation of laser stimulation (pre-stimulus EEG activity: −500 to 0 ms), and the other population consisted of EEG recordings after the presentation of laser stimulation of the same trial (post-stimulus EEG activity: 0 to 500 ms, where the Aδ related LEP responses were dominantly observed). The pre- and post-stimulus EEG activities over all channels of the same trial formed two matrices $\mathbf{X}_{pre}, \mathbf{X}_{post} \in \mathbb{R}^{N \times T}$, where N is the number of channels and T is the number of samples in each trial. To maximize the difference between the variance of $\mathbf{X}_{pre}$ and $\mathbf{X}_{post}$, CSP is objective to estimate the generalized eigenvector or the projection vector $\mathbf{w}$ by solving the generalized eigenvalue problem as follows:

$$\left\langle \mathbf{X}_{post}\mathbf{X}_{post}^{T} \right\rangle \mathbf{w} = \lambda \left\langle \mathbf{X}_{pre}\mathbf{X}_{pre}^{T} \right\rangle \mathbf{w}, \tag{1}$$

where $\langle\cdot\rangle$ is the averaging operator across trials for the same population and λ is the generalized eigenvalue. The matrix $\mathbf{W} = [\mathbf{w}_1, \cdots, \mathbf{w}_N] \in \mathbb{R}^{N \times N}$, where $\mathbf{w}_1, \cdots, \mathbf{w}_N$ are N eigenvectors estimated from Eq. (1), is the spatial filter, and $\mathbf{A} = \mathbf{W}^{-1} \in \mathbb{R}^{N \times N}$ is the spatial pattern represented as a weighting of EEG channels. Importantly, CSP provided an ordered list of spatial patterns according to the discriminative power between two populations. As a result, the spatial pattern with the maximal variance of $\mathbf{X}_{post}$ would capture the minimal variance of $\mathbf{X}_{pre}$, and vice versa. Typically, only a few spatial patterns were sufficient for the discrimination

between two populations (Muller-Gerking et al., 1999). These few spatial patterns, which can isolate stimulus-evoked EEG responses (contained only in $\mathbf{X}_{post}$) from spontaneous EEG activity (contained in $\mathbf{X}_{post}$ as well as $\mathbf{X}_{pre}$), worked as an effective spatial filter. In the present study, three eigenvectors corresponding to the largest eigenvalues of $\mathbf{X}_{post}$ and lowest eigenvalues of $\mathbf{X}_{pre}$ were selected to reconstruct spatial-filtered single-trial EEG responses of all channels (see Section 1 in the Supplementary Materials for the reason of selecting three CSP components).

Multiple linear regression

To estimate single-trial LEP features automatically and reliably, we applied a multiple linear regression method (Mayhew et al., 2006) to LEP trials recorded at Cz within the post-stimulus time interval (0 to 500 ms), which were filtered using the combination of BPF, ICA, and CSP. The MLR approach takes into account the variability of both N2 and P2 latency and amplitude of LEPs, and models single-trial LEP responses as follows:

$$f(t) = a_N y_N(t + l_N) + a_P y_P(t + l_P), \tag{2}$$

where $f(t)$ is a modeled single-trial LEP waveform that varies as a function of time t, $y_N(t)$ and $y_P(t)$ are the templates of N2 and P2 waves, which can generally be obtained as the average of all LEP trials of each participant, a_N and a_P are the weights of N2 and P2 templates, and l_N and l_P are the latency shift values of the N2 and P2 templates, respectively. Since the N2 and P2 peaks of the LEPs reflect the activity of the different neural generators (Garcia-Larrea et al., 2003), and their amplitudes can be differentially modulated by several experimental factors (e.g., spatial attention and probability of perception) (Lee et al., 2009; Legrain et al., 2002), we modeled the N2 and P2 waves separately, thus avoiding the assumption that all generators contributing to the LEP responses covary linearly (Hu et al., 2011). Using the Taylor expansion, the MLR model can be written as follows:

$$\begin{aligned} f(t) &\approx a_N y_N(t) + l_N a_N y'_N(t) + a_P y_P(t) + l_P a_P y'_P(t) + \varepsilon \\ &= \beta_1 y_N(t) + \beta_2 y'_N(t) + \beta_3 y_P(t) + \beta_4 y'_P(t) + \beta_5, \end{aligned} \tag{3}$$

where $y'_N(t)$ and $y'_P(t)$ are the temporal derivatives of N2 and P2 templates, respectively, and ε is the residual term. Thus the single trial LEP waveform is approximated using the sum of the weighted averages of N2 and P2 templates and their respective temporal derivatives. Considering that these weights ($\beta_1, \beta_2, \beta_3, \beta_4, \beta_5$) captured the single-trial variability of N2 and P2 latency and amplitude in LEPs, these coefficients could be closely related to the subjective intensity of pain perception. Correlations between these estimated single-trial coefficients and the corresponding single-trial ratings of pain perception were measured using Pearson's correlation coefficient for each participant (Hu et al., 2011). The obtained correlation coefficients were transformed to Z values using the Fisher R-to-Z transformation and were finally compared against zero using a one-sample t-test.

Performance evaluation

To quantitatively assess the performance of each analysis step (BPF, ICA, CSP, and MLR) for enhancing the SNR of single-trial LEPs, raw data, and denoised data after each analysis step were evaluated using a similarity index (SMI) (Su et al., 2012), which is the power ratio between the "LEP-like" data in a testing trial and the residual. Let $\bar{z}$ be the average of training trials and z_k be the kth testing trial, and the SMI is calculated as follows:

$$\mathrm{SMI} = 10\log_{10}\left(\frac{\sigma^2(P)}{\sigma^2(R)}\right), \tag{4}$$

where $P = \frac{\bar{z}^T z_k}{\bar{z}^T \bar{z}}\bar{z}$ is the orthogonal projection of z_k on to $\bar{z}$, and $R = z_k - P$ is the residual part. A large SMI indicates that the testing trial z_k is similar to the average $\bar{z}$ of training trials, and vice versa. Since SMI is sensitive to the average response of training trials, the control of its quality is achieved in the following two aspects:

First, BPF, ICA, and CSP were only performed on single-trial LEP responses, which indicated that these analysis steps did not result in a test trial similar to the average response of training trials (i.e., not sensitive to the average response). Indeed, only the last analysis step, MLR, was sensitive to the average response of training trials, as the average response was used as the model to fit the response of test trial. Second, the quality of average response was greatly improved from the former three analysis steps (BPF, ICA, and CSP), that allowed to remove the majority of artifacts from single-trial LEP responses. The average responses of training trials with improved SNR were used in the MLR analysis.

SMI values calculated from all data were compared using a 5-level (raw data, data after BPF, data after ICA, data after CSP, and data after MLR) one-way repeated-measures ANOVA. When the main effect of the ANOVA was significant ($p < 0.05$), post hoc pairwise comparisons (two-sample t-test) were performed.

Prediction of pain perception

Based on the estimated MLR coefficients β_1, β_2, β_3, β_4 and β_5, we (1) discretely predicted the intensity of pain perception by classifying EEG trials into two levels (low pain: VAS < 5, high pain: VAS ≥ 5) using a Naïve Bayes classifier, and (2) continuously predicted the intensity of pain perception for each EEG trial within the scale range from 0 to 10 using a multiple linear prediction model. Both the binary (classification of low pain and high pain) and continuous (regression on a continuous scale from 0 to 10) prediction of pain perception was performed at the within- and cross-individual levels. Note that all five MLR coefficients (β_1, β_2, β_3, β_4, and β_5) were used as LEP features for the prediction of pain perception since the use of all five coefficients contributed to the (almost) best prediction performance (see Section 2 in the Supplementary Materials for details about the feature selection). Note also that at cross-individual level, both single-trial LEP features (MLR coefficients) and single-trial ratings of pain perception were normalized to minimize the commonly observed inter-individual variability. For each participant, single-trial LEP features were normalized by subtracting the mean and dividing by the standard deviation (i.e., represented as z values), and single-trial ratings of pain perception were rescaled within the range from 0 to 10 (defining 0 as the lowest pain rating and 10 as the highest pain rating for each participant).

Binary prediction: classification of low pain and high pain

LEP trials were divided into two groups: training trials and test trial(s) (see Cross validation section for details). Training trials were divided into two categories (labeled as low pain: VAS < 5, and high pain: VAS ≥ 5) according to the pain perception ratings for each participant. The MLR coefficients β_1, β_2, β_3, β_4 and β_5 were extracted from both training and testing trials, and were used as LEP features for subsequent classification. A Naïve Bayes classifier (Witten and Hall, 2011) was first trained with single-trial LEP features (i.e., five MLR coefficients) of training trials (to code the relationship between single-trial LEP features and the corresponding labels of pain perception), and then applied to the test trial(s) to predict single-trial labels from the corresponding single-trial LEP features.

It's well known that the Naïve Bayes classifier was capable of providing an accurate classification even with a small number of training data (Witten and Hall, 2011; Zhang, 2004). Therefore, it is particularly

suitable for the present study, since the number of LEP trials was limited for each individual. A comparison between the Naïve Bayes and other popular classifiers, such as linear discriminant analysis (Duda et al., 2000) and support vector machine (Cortes and Vapnik, 1995), was summarized in Section 3 of the Supplementary Materials.

The prediction performance was evaluated using the classification accuracy, i.e., the percentage of accurate predictions. In addition, to demonstrate that the larger the difference of VAS between categories, the higher the classification accuracy, and vice versa, we performed several binary predictions to distinguish multiple categories of pain perception at within-individual level, which were summarized in Section 4 of the Supplementary Materials.

Continuous prediction: regression of pain perception intensity

A linear regression analysis was adopted to model the relationship between single-trial LEP features and the corresponding intensity of pain perception for continuous prediction of the pain perception from the LEP features. For the kth training trial, the linear regression model can be written as follows:

$$I_k = \sum_{i=1}^{5} \alpha_i \beta_{ik} + c, \tag{5}$$

where I_k is the intensity of pain perception, β_{ik} ($i = 1, 2, \ldots, 5$) are the LEP features (i.e., MLR coefficients) extracted from Eq. (3), and α_i and c are the coefficients of linear regression model, which were estimated using the ordinary least squares method. Following, the generated linear regression model was applied to the test trial(s) to predict the single-trial intensity of pain perception from the corresponding single-trial LEP features. A comparison between ordinary least squares and other methods (such as lasso and ridge) (Tibshirani, 1996) was summarized in Section 5 of the Supplementary Materials.

The prediction performance was evaluated using the Mean Absolute Error (MAE), which can be written as follows:

$$\mathrm{MAE} = \frac{1}{N} \sum_{n=1}^{N} \left| I_n - \hat{I}_n \right|, \tag{6}$$

where I_n and $\hat{I}_n$ are the real and predicted intensity of pain perception for trial n, and N is the number of trials of each participant for within-individual prediction, or of all participants for cross-individual prediction. The MAE represented the absolute difference between the predicted values and real values in linear regression analysis, and it served as a straightforward measure on how close the predicted values were to the real intensity of pain perception in the present study.

Cross validation

Leave-one-out cross validation (LOOCV) (Duda et al., 2000) was used in two stages of data analysis: (1) single-trial LEP feature extraction (CSP and MLR) and (2) prediction of pain perception (Naïve Bayes classifier and linear regression model). For example, when we perform CSP analysis, the spatial filter was obtained from all training trials, and applied to both training and test trials to enhance their SNRs.

It should be noted that different LOOCV strategies were adopted to predict pain perception at both the within- and cross-individual levels. In the present study, there were 29 participants with 40 LEP trials each. At the within-individual level, LOOCV was achieved by dividing 40 LEP trials into 39 training trials and 1 test trial, and the same procedure was repeatedly performed 40 times to make sure that each LEP trial was used as the test trial once. At the cross-individual level, LOOCV was achieved by dividing 29 subjects into 28 training subjects and 1 test subject, and similarly, the same procedure was repeatedly performed 29 times to make sure that each subject was used as the test subject once (all LEP trials from this subject were used as test trials). Considering the substantial inter-individual variability of both LEP features and pain perception (e.g., one participant has high LEP responses and low pain perception, while another participant may have low LEP responses and high pain perception), both single-trial LEP features and single-trial ratings of pain perception intensity were normalized for each participant at the cross-individual level. The comparison of prediction performance with and without the normalization of both single-trial LEP features and single-trial ratings of pain perception was summarized in Section 6 of the Supplementary Materials.

Comparison between binary prediction and continuous prediction

To compare the reliability of binary and continuous prediction methods, a unifying measure, named Proportional Reduction in Loss (PRL) (Cooil and Rust, 1994; Rust and Cooil, 1994), is calculated as:

$$PRL = (E_{max} - E)/E_{max}, \tag{7}$$

where E is the expected loss, which can be estimated from the classification accuracy in binary prediction, and from MAE in continuous prediction, and E_{max} is the maximum possible expected loss, where the prediction is completely unreliable (i.e., at the chance level). A perfectly correct prediction would have the loss $E = 0$, then $PRL = 1$. In contrast, a completely unreliable prediction would have the loss $E = E_{max}$, then $PRL = 0$. That is, the higher the PRL, the more reliable the prediction.

For binary prediction (two-class classification), we have $E_{max} = 50\%$ and $E = 100\% - accuracy(\%)$. For continuous prediction, E is the MAE value of the linear regression and E_{max} is the MAE value calculated when the prediction is totally random, which is realized by resampling without replacement. Specifically, E_{max} is calculated by the following steps: (i) randomly assigning one value within 0–10, representing the predicted pain perception intensity, to each single trial for each participant; (ii) calculating the MAE value from the randomly assigned values of all 40 trials for each participant; and (iii) repeating steps (i) and (ii) for 100 times for each participant, and calculating the average MAE value (i.e., E_{max}).

Results

Laser-evoked brain responses

Laser stimuli elicited a clear pinprick perception and reproducible time-locked LEPs in all participants (mean VAS = 5.8 ± 1.2), related to the activation of Aδ fibers (Bromm and Treede, 1984). Fig. 2 shows the group-level average LEP waveforms at Cz (nose reference) and the scalp topographies of N2 and P2 waves for each level of pain perception intensity (I1–I4). Across subjects, latencies and amplitudes of N2 and P2 peaks for each level of pain perception intensity were as follows: N2 latency (I1: 256 ± 19 ms, I2: 230 ± 23 ms, I3: 204 ± 35 ms, I4: 198 ± 51 ms; $F = 16.5$, $p < 0.001$); N2 amplitude (I1: −11 ± 7 μV, I2: −22 ±13 μV, I3: −32 ± 15 μV, I4: −43 ± 16 μV; $F = 27.94$, $p < 0.001$); P2 latency (I1: 338 ± 33 ms, I2: 350 ± 37 ms, I3: 356 ± 36 ms, I4: 364 ± 45 ms, $F = 2.36$, $p = 0.075$); P2 amplitude (I1: 8 ± 5 μV, I2: 16 ± 9 μV, I3: 26 ± 11 μV, I4: 33 ± 9 μV; $F = 39.94$, $p < 0.001$). Scalp topographies of the N2 and P2 waves were markedly similar across four levels of pain perception intensity. Consistent with previous studies (Kunde and Treede, 1993; Valentini et al., 2012), the N2 wave extended bilaterally towards temporal regions, whereas the P2 wave was more centrally distributed.

Single trial LEP features

The procedure to enhance the SNR of single-trial LEP responses was illustrated in Fig. 3. First, a 1–30 Hz bandpass filter was applied to both resting EEG and LEP responses (both training and test trials) for effectively attenuating low- and high-frequency artifacts (Fig. 3, top panel;

step 1). Then, ICA algorithm was applied to the bandpass filtered training trials for correcting EEG trials that contaminated by eye-blinks and movements (Fig. 3, top panel; step 2). Following, CSP algorithm was applied on ICA corrected resting EEG and LEP responses (pre- and post-stimulus EEG activities respectively) to extract a few spatial patterns that can maximally differentiate LEP responses from spontaneous EEG activity (Fig. 3, top panel; step 3). Next, MLR algorithm was applied on CSP refined resting EEG and LEP responses to model the variability of single-trial latency and amplitude of N2 and P2 waves, which could not only enhance the SNR of single-trial LEP responses, but also provide an effective way to parameterize single-trial LEP responses using five MLR coefficients (β_1, β_2, β_3, β_4, and β_5) (Fig. 3, top panel; step 4). All filter models (ICA, CSP, and MLR models) that generated from training trials, were subsequently applied on the test trial(s) (Fig. 3, right part of the top panel).

In the bottom panel of Fig. 3, we show how these filters significantly enhanced the SMI step by step (raw data: -8.7 ± 5.4, data after BPF: -7.6 ± 4.6, data after ICA: -6.5 ± 4.6, data after CSP: -4.7 ± 4.0, data after MLR: -0.7 ± 3.3; $F = 79.24$, $p = <0.001$). Post hoc comparison revealed that (1) the enhancement of SMI from raw data to data after CSP was significant ($p < 0.05$), and (2) the enhancements of SMI from raw data, data after BPF, data after ICA, and data after CSP to data after MLR were all significant ($p < 0.05$ for all comparisons). Note that the increase of SMI, which indicated the ratio between "LEP-like" responses (signal) and "LEP-irrelevant" residual (noise), quantified the performance of tested filters to enhance the SNR.

Fig. 4 shows the correlations between single-trial LEP features (MLR coefficients: β_1, β_2, β_3, and β_4), estimated using MLR algorithm, and the corresponding intensity of pain perception. Both β_1 and β_3, which captured the variability of single-trial N2 and P2 amplitudes respectively, were significantly and strongly correlated with the corresponding intensity of pain perception (β_1: mean $R = 0.74$, $p < 0.001$; β_3: mean $R = 0.52$, $p < 0.001$). In addition, both β_2 and β_4, which captured the variability of single-trial N2 and P2 latencies respectively, were significantly but weakly correlated with the corresponding intensity of pain perception (β_2: mean $R = 0.34$, $p < 0.001$; β_4: mean $R = 0.28$, $p < 0.001$). As expected, β_5, which captured the variability of residual noise, was not significantly correlated with the corresponding intensity of pain perception (β_5: mean $R = 0.04$, $p = 0.176$).

Binary prediction: classification of low pain and high pain

Table 1 summarized the classification accuracy for binary prediction of low pain and high pain using MLR coefficients. Two-way repeated measures ANOVA to assess the effect of classification scenarios (factor 1: within- and cross-individual levels) and LEP features (factor 2: β_1, β_2, β_3, β_4, β_5, and all MLR coefficients) on prediction accuracy revealed that (1) the prediction accuracy was significantly different using different classification scenarios ($F = 79.25$, $p < 0.001$), with higher accuracy for prediction at within-individual level than at cross-individual level; (2) the prediction accuracy was significantly different using different LEP features ($F = 28.29$, $p < 0.001$); and (3) there was no significant interaction between the two factors ($F = 1.856$, $p = 0.140$). At within-individual level, post hoc analysis revealed that the prediction accuracy was significantly higher for β_1 than β_2, β_4, and β_5 ($p = 0.007$, $p = 0.014$, and $p = 0.002$ respectively); for β_3 than β_5 ($p = 0.041$); for all MLR coefficients than β_2, β_3, β_4, and β_5 ($p = 0.002$, $p = 0.021$, $p = 0.004$, and $p = 0.001$ respectively). At the cross-individual level, post hoc analysis revealed the prediction accuracy was significantly higher for β_1 than β_2, β_4, and β_5 ($p < 0.001$ for all comparisons); for β_3 than β_2, β_4, and β_5 ($p < 0.001$ for all comparisons); for all MLR coefficients than β_2, β_3, β_4, and β_5 ($p < 0.001$, $p = 0.011$, $p < 0.001$, and $p < 0.001$ respectively).

A comprehensive comparison of classification accuracy using all possible combinations of MLR coefficients was provided in Section 2 of the Supplementary Materials.

Continuous prediction: regression of pain perception intensity

The prediction of pain perception intensity using linear regression model at both within- and cross-individual levels was shown in Fig. 5. Across participants, MAE values were 1.031 ± 0.136 and 1.821 ± 0.202 for within-individual and cross-individual levels, respectively. The probability density distribution of prediction error indicated that the 50% and 95% error intervals were respectively [−0.890, 0.699] and [−2.685, 2.943] at within-individual level, and were respectively [−1.591, 1.530] and [−4.270, 4.626] at cross-individual level. It should be noted that, at cross-individual level, single-trial MLR coefficients and single-trial ratings of pain perception intensity were normalized for each participant, which made it impossible to directly compare the prediction performance (indexed by MAE values) between within-individual and cross-individual levels.

To statistically compare their prediction performance, single-trial ratings of pain perception were rescaled within the range from 0 to 10 (defining 0 as the lowest pain rating and 10 as the highest pain rating for each participant) after prediction for pain prediction at within-individual level. The same scaling, calculated from real single-trial ratings of pain perception, was applied on predicted single-trial ratings. After rescaling, the MAE values were 1.607 ± 0.207 across participants for pain prediction at within-individual level, which was significantly lower than those at cross-individual level (1.821 ± 0.202; $p < 0.001$, paired sample t-test).

Comparison between binary prediction and continuous prediction

At within-individual level, the PRL values for binary and continuous predictions were respectively 0.73 ± 0.17 and 0.52 ± 0.08 ($p < 0.001$, paired two-sample t-test). The result indicated that continuous prediction could provide a prediction of pain perception intensity at a finer scale than binary prediction (continuous value from 0 to 10 vs. either low or high pain), while binary prediction is significantly more reliable than continuous prediction.

Discussion

In the present study, we aimed at developing a fast, automated, and reliable approach for (1) estimating single-trial LEP features and (2) predicting pain perception from estimated single-trial LEP features. We applied a novel single-trial analysis approach that combined CSP and MLR to automatically and reliably estimate single-trial LEP features, and adopted a Naïve Bayes classifier to discretely predict low and high pain and a multiple linear prediction model to continuously predict the intensity of pain perception from single-trial LEP features, at both within- and cross-individual levels. Our results showed that the proposed approach provided a binary prediction of pain (classification of low pain and high pain) with an accuracy of $86.3 \pm 8.4\%$ (within-individual) and $80.3 \pm 8.5\%$ (cross-individual), and a continuous prediction of pain (regression on a continuous scale from 0 to 10) with an MAE value of 1.031 ± 0.136 (within-individual) and 1.821 ± 0.202 (cross-individual). Considering the good performance of the proposed approach in various pain prediction scenarios, this study may help establish a fast and reliable tool for automated prediction of pain, which could be potentially adopted in various basic and clinical applications.

Pain prediction: technical notes and improvements

A practically useful tool to predict pain perception of humans should be sufficiently rapid, accurate, and automatic, in order to satisfy the requirement of most real-world applications. To achieve these goals, our study proposed a novel and practice-oriented strategy of pain prediction, which showed several distinctions as compared with previous studies on pain prediction (Brodersen et al., 2012; Bromm and Treede, 1991; Marquand et al., 2010; Prato et al., 2011; Schulz et al., 2012).

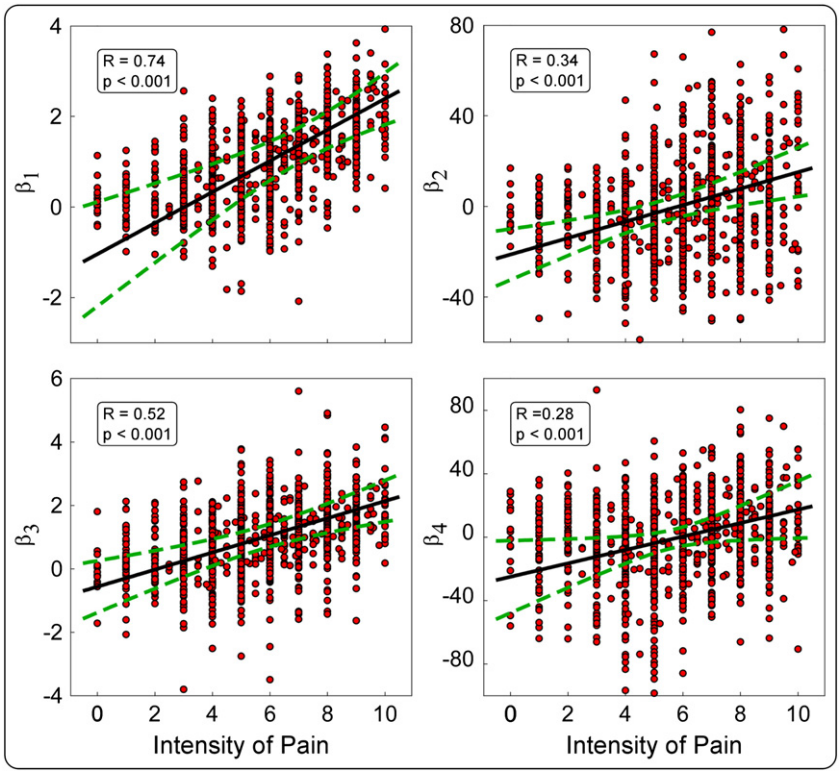

Fig. 4. Correlations between single-trial MLR coefficients (β_1, β_2, β_3 and β_4) and intensity of pain perception. Both β_1 and β_3 significantly correlated with the intensity of pain perception (β_1: mean R = 0.74, p < 0.001; β_3: mean R = 0.52, p < 0.001). Both β_2 and β_4 significantly (but relatively weakly as compared with β_1 and β_3) correlated with the intensity of pain perception (β_2: mean R = 0.34, p < 0.001; β_4: mean R = 0.28, p < 0.001). The black solid lines and green dash lines represent the mean and SD of the best linear fit across participants.

The possibility of pain prediction using non-invasive neuroimaging techniques was first explored by several research groups using functional magnetic resonance imaging (fMRI) (Brodersen et al., 2012; Brown et al., 2011; Marquand et al., 2010; Prato et al., 2011). Because of the high spatial resolution, whole-brain fMRI technique could not only reveal spatially distributed patterns of activity underlying specific perceptual, cognitive states (Brodersen et al., 2012; Marquand et al., 2010; Raij et al., 2005), but also provide a prediction of pain perception with a relatively high accuracy (Brown et al., 2011; Marquand et al., 2010). At within-individual level, Marquand et al. (2010) was able to classify three levels of painful stimuli with a prediction accuracy ranging from 68.3% to 91.7%. At cross-individual level, Brown et al. (2011) reported an averaged classification accuracy of 86.6% to distinguish nonpainful and painful stimuli. Note that, as compared with the fMRI-based pain prediction studies, we have obtained quite comparable results using EEG technique in the present study (at within- and cross-individual levels, respectively, a prediction accuracy of 86.3 ± 8.4 and 80.3 ± 8.5 to classify low- and high pain, and an MAE of 1.031 ± 0.136 and 1.821 ± 0.202 to regress pain perception on a continuous scale from 0 to 10). Importantly, as compared with fMRI, EEG was much less expensive, portable, and widely equipped in hospitals, clinics, and research units (Hüsing et al., 2006). Thus, EEG-based pain prediction is more convenient and feasible for practical applications.

Along with the functional magnetic resonance imaging-based studies, Schulz et al. (2012) first described the use of single-trial multi-channel EEG recordings to classify low and high pain and to predict the individual sensitivity to pain. A multivariate pattern analysis strategy has been adopted in all these EEG- or fMRI-based pain prediction studies, since multivariate pattern analysis holds the unique advantage of being able to reveal important pattern information jointly presented by a number of variables (spatial pattern in fMRI, temporal and time–frequency patterns in EEG) and thus is free of the sophisticated feature extraction process (O'Toole et al., 2007). However, such a multivariate pattern analysis strategy usually had an extremely high computational complexity (O'Toole et al., 2007), and could not provide an effective prediction of pain in practical applications. To provide a rapid and reliable prediction of pain from single-trial EEG recordings, we proposed to build the classifier and regression model using LEP features that (1) showed a strong correlation with subjective pain perception and (2) captured a high SNR, instead of using all available EEG samples in the multivariate pattern analysis strategy. Among all explored LEP features (i.e., N1, N2, and P2 waves, event-related desynchronization at alpha band and gamma band oscillations), N2 and P2 waves captured the highest SNR, and the strongest correlation with subjective pain perception (Iannetti et al., 2008; Zhang et al., 2012). Therefore, N2 and P2 waves were the most commonly used measurements to assess LEPs in clinical practice, while other LEP features were restricted in clinical recommendations (Cruccu et al., 2008; Treede et al., 2003). In the present study, we have followed the clinical LEP recommendations, and proposed an innovative single-trial analysis approach to enhance the SNR of LEP responses and to parameterize N2 and P2 related LEP features (i.e., MLR coefficients that coded the single-trial variability of N2 and P2 latency and amplitude)

Table 1
Classification accuracy for binary prediction of low pain and high pain using each of MLR coefficients and all MLR coefficients.

	MLR coefficients					
	β_1 (%)	β_2 (%)	β_3 (%)	β_4 (%)	β_5 (%)	All (%)
Within-individual	85.2 ± 9.4	74.6 ± 14.7	79.7 ± 12.1	74.2 ± 17.1	70.6 ± 19.3	86.3 ± 8.4
Cross-individual	78.8 ± 10.3	55.1 ± 13.5	74.0 ± 10.0	58.3 ± 13.2	55.9 ± 12.6	80.3 ± 8.5

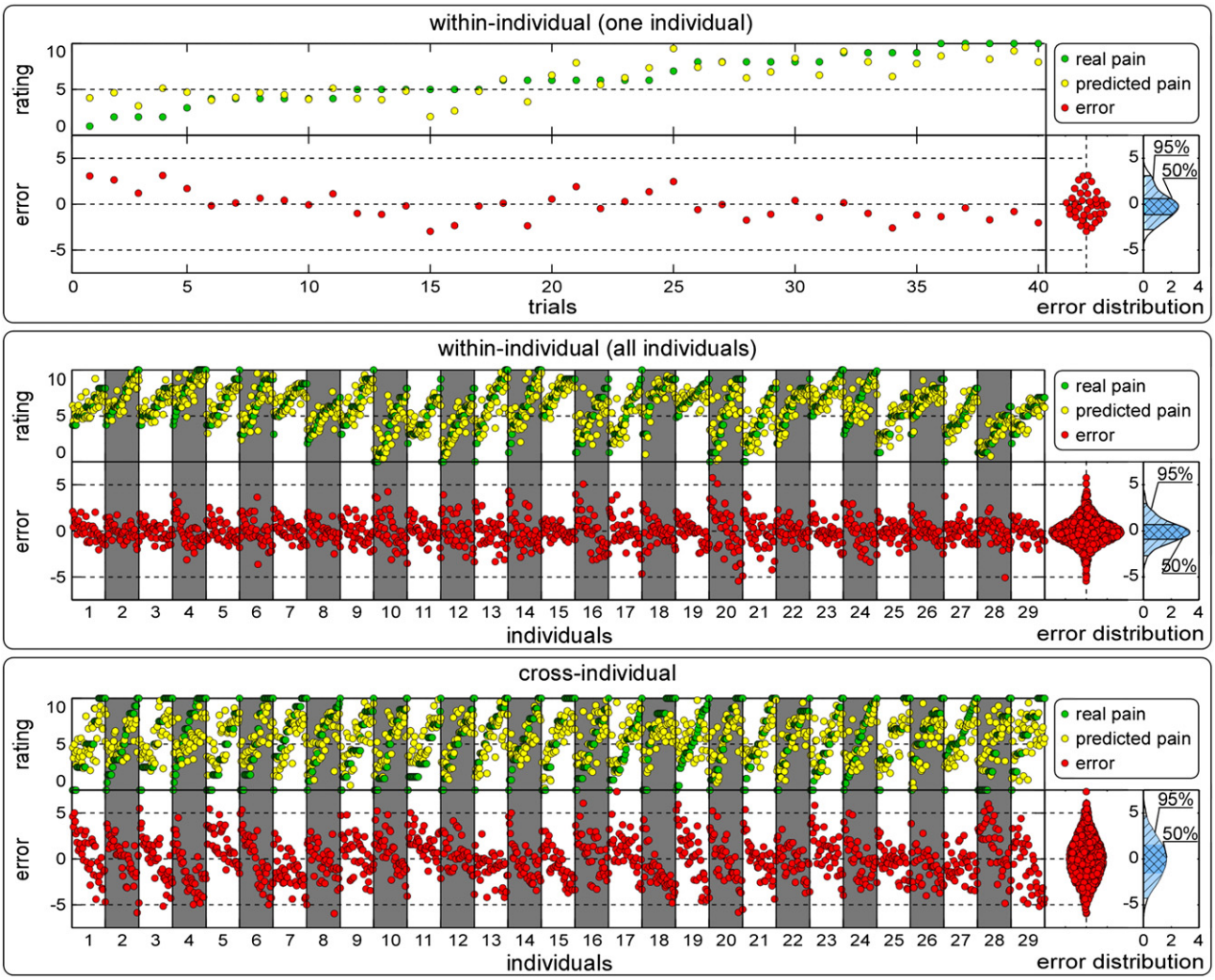

Fig. 5. The prediction of intensity of pain perception using linear regression model at both within- and cross-individual levels. Dots in green, yellow, and red indicate the real intensity of pain perception, predicted intensity of pain perception, and the prediction error. Trails were sorted according to the real intensity of pain perception to better the visualization (increase from left to right). Top panel: The prediction performance of linear regression model for within-individual strategy of a representative participant (MAE = 1.205). The probability density distribution of prediction error indicated that the 50% and 95% error intervals were respectively [−1.153, 0.590] and [−2.792, 3.092]. Middle panel: The prediction performance of linear regression model for within-individual strategy of all participants (MAE = 1.031 ± 0.136). The probability density distribution of prediction error indicated that 50% and 95% error intervals were respectively [−0.890, 0.699] and [−2.685, 2.943]. Bottom panel: The prediction performance of linear regression model for cross-individual strategy of all participants (MAE = 1.821 ± 0.202). The probability density distribution of prediction error indicated that 50% and 95% error intervals were respectively [−1.591, 1.530] and [−4.270, 4.626].

(Figs. 3 and 4). Such single-trial analysis approach (the combination of BPF, ICA, CSP, and MLR) could not only significantly improve the SNR of single-trial LEP waveforms (Fig. 3, bottom panel; $F = 79.24$, $p < 0.001$), but also be executed rapidly and automatically, thus avoiding any bias due to manual operation. It should be noted that the performance of ICA and CSP depends on the number of channels and the layout, and we have provided evidence showing that the proposed single-trial analysis achieved a good performance using the 64-channel montage on the extended 10–20 system. Montage with fewer channel, preferable in clinical application, would be evaluated in our future study. In addition, the proposed framework to predict pain could be adapted for predicting subjective sensation from event-related potentials in various sensory modalities.

Pain prediction: physiological considerations

Many studies contributed to revealing the physiological significance of brain activations after the presentation of nociceptive stimulus (e.g., intensive laser stimulation) (Apkarian et al., 2005; Baumgärtner et al., 2010; Brooks and Tracey, 2005; Davis and Moayedi, 2012; Garcia-Larrea et al., 2003; Tracey and Mantyh, 2007). However, brain response and brain area that specifically respond to pain have not been unveiled (Davis et al., 2012; Mouraux and Iannetti, 2009). On one hand, brain activations to nociceptive stimulus were functionally similar to other brain responses elicited by intense stimuli belonging to non-nociceptive sensory modalities (e.g., tactile, auditory, and visual) (Mouraux et al., 2011; Mouraux and Iannetti, 2009). On the other hand, brain areas showing activation to nociceptive stimulus were also associated with non-nociceptive sensory functions and high-level cognitions (e.g., attention, salience) (Davis, 2006; Davis et al., 2000; Downar et al., 2003; Legrain et al., 2011). The fact that non-nociceptive neurons are intermingled with and possibly outnumber nociceptive neurons even in brain areas that respond to nociceptive stimulus (Davis et al., 2012; Kenshalo et al., 2000) hampered the exploration of nociceptive-specific brain areas and responses. We are aware that N2 and P2 waves in LEPs are functionally similar to other vertex potentials elicited by intense stimuli belonging to non-nociceptive sensory modalities (Mouraux and Iannetti, 2009) and largely reflect saliency-related neural processes possibly related to the detection of relevant changes in the sensory environment (Downar et al., 2000). Therefore, even if we have achieved a relatively high accuracy to predict pain perception (Table 1 and Fig. 5), the present study does not claim to make any

progress of establishing an objective neuronal marker of pain perception. Note that the gamma band oscillations, which we have previously proven to have a close relationship with pain perception (regardless of stimulus repetition) (Zhang et al., 2012), normally have a very low SNR, thus not suitable for such a practice-oriented strategy of pain prediction at the current stage.

Bear in mind that, in clinical applications, N2 and P2 waves in LEPs are recommended to diagnose the deficit of the nociceptive system (e.g., lesions in spinal root) (Treede et al., 2003). Identical to this principle, the use of N2 and P2 waves in LEPs to predict the subjective pain perception possesses important clinical significance (e.g., to monitor the effect of analgesic drug or the recovery of nociceptive system for non-communicative patients). Importantly, a careful experimental protocol design (e.g., a sufficiently long and variable ISI; for example, an ISI larger than 10 s and varied randomly across trials) should be required during the EEG recording to rule out any possible intra-individual variability (e.g., attention, habituation, and negative emotion), other than subjective pain perception, coded by single-trial LEP waveforms.

As correctly stated in previous studies, the pain prediction at cross-individual level (a classifier and/or a regression model was trained on a group of individuals and applied on another individual) would be needed in most practical applications (Brodersen et al., 2012; Schulz et al., 2012). However, because of the inherent inter-individual differences (inter-individual variability) of the brain structure and function (especially for pain perception, or say, pain is unique for each individual), a tailored approach, which incorporates individual factors that are particularly related to inter-individual variability of pain perception into the pain prediction model, could be the ultimate solution in pain research and pain therapy (Davis, 2011). If the pain prediction is performed at cross-individual level, we would completely ignore individual peculiarities, which are particularly serious for highly sensitive contexts, e.g., pain perception (Brodersen et al., 2012). The direct consequence of ignoring inter-individual variability is the inaccuracy prediction of pain perception (i.e., prediction bias), normally showing a higher predicted pain for low real pain and/or a lower predicted pain for high real pain (Supplementary Fig. 3; MAE $= 2.573 \pm 0.259$). If the pain prediction was performed on a within-individual level, we would unavoidably need the real pain ratings for each individual, which implies that such pain prediction strategy cannot be used in some real-world applications (e.g., for non-communicative patients).

The intuitive solution to minimize such discrepancy would be reducing the inter-individual variability through normalization for both LEP features and ratings of pain perception. In the present study, for each participant, single-trial LEP features were normalized by subtracting the mean and dividing by the standard deviation (i.e., represented as z values), and single-trial ratings of pain perception intensity were rescaled within the range from 0 to 10 (defining 0 as the lowest pain rating and 10 as the highest pain rating for each participant). Such normalization could significantly increase the prediction accuracy (Supplementary Fig. 3; MAE values before and after normalization were respectively 2.573 ± 0.259 vs. 1.821 ± 0.202; $p < 0.05$). Indeed, such inter-individual variability cannot be completely removed using normalization (after rescaling of pain perception intensity from 0 to 10, MAE values at within- and cross-individual levels were respectively 1.607 ± 0.207 and 1.821 ± 0.202; $p < 0.001$). In summary, whereas a pain prediction at within-individual level could have a high prediction accuracy but less clinically applicable, a pain prediction at cross-individual level cannot be very accurate due to the intrinsic inter-individual variability. Normalization of LEP features and ratings of pain perception, serving as a tradeoff between the above explained discrepancy, could reduce the level of inter-individual variability and provide a more accurate prediction of pain perception. This strategy (normalization) could be adopted when the subjective pain perception ratings of the tested individual are not available and the difference of brain structure/function between the tested individual and norm collective is large enough (e.g., for non-communicative patients).

As explained above, both intra- and inter-individual variability, instead of the contaminated noise in the recorded neural responses, could intrinsically hamper our pursuit of a sufficiently high accuracy of pain prediction. In addition to exploring the pain-specific neural responses and controlling the experimental protocol to minimize the intra-individual variability, as well as adopting normalization to minimize the inter-individual variability, we may need to incorporate various physiological (e.g., heart rate and body temperature) and trait-based measurements (fear of pain and pain catastrophizing) to achieve a higher pain prediction accuracy (Brown et al., 2011; Ochsner et al., 2006; Seminowicz and Davis, 2006; Tousignant-Laflamme et al., 2005; Zwakhalen et al., 2006).

Conclusions

In the present study, we proposed a practice-oriented EEG-based pain prediction strategy, which adopted single-trial analysis to estimate LEP features for an effective pain prediction. Such analytical strategy could be executed rapidly, reliably, and automatically, thus satisfying most requirements of various basic and clinical applications. In addition, we have performed pain prediction with various scenarios (e.g., binary two-level classification and continuous linear regression, as well as pain prediction at within- and cross-individual levels) to achieve a comprehensive understanding of practical issues of pain prediction. A careful experimental protocol design should be followed to minimize the intra-individual variability (e.g., variability of attention, negative emotion for the same individual), and a normalization strategy should be adopted to minimize the inter-individual variability (i.e., individual peculiarities). All these improvements could thereby potentially help optimize the prevention, diagnosis, monitoring, and treatment of pain for non-communicative patients and patients with disorders of consciousness (Schnakers et al., 2010; Schulz et al., 2012).

Acknowledgments

LH and PX were supported by the National Natural Science Foundation of China (31200856), Natural Science Foundation Project of CQ CSTC, Special Financial Grant from the China Postdoctoral Science Foundation (2012T50755), and New Teacher Fund of Ministry of Education of China (20120182120002). GH, YSH and ZGZ were partially supported by a Grant (HKU 762111M) from the Hong Kong SAR Research Grants Council and a Grant (201211159074) from HKU CRCG. The collaboration between LH and GDI is generously supported by the IASP® Developed-Developing Countries Collaborative Research Grant.

Conflict of interest

All authors have no conflict of interest.

Appendix A. Supplementary Materials

Supplementary data to this article can be found online at http://dx.doi.org/10.1016/j.neuroimage.2013.05.017.

References

Apkarian, A.V., Bushnell, M.C., Treede, R.-D., Zubieta, J.-K., 2005. Human brain mechanisms of pain perception and regulation in health and disease. Eur. J. Pain 9, 463–484.
Aslaksen, P.M., Myrbakk, I.N., Hoifodt, R.S., Flaten, M.A., 2007. The effect of experimenter gender on autonomic and subjective responses to pain stimuli. Pain 129, 260–268.
Baumgartner, U., Cruccu, G., Iannetti, G.D., Treede, R.D., 2005. Laser guns and hot plates. Pain 116, 1–3.
Baumgärtner, U., Iannetti, G.D., Zambreanu, L., Stoeter, P., Treede, R.-D., Tracey, I., 2010. Multiple somatotopic representations of heat and mechanical pain in the operculo-insular cortex: a high-resolution fMRI study. J. Neurophysiol. 104, 2863–2872.
Blankertz, B., Losch, F., Krauledat, M., Dornhege, G., Curio, G., Muller, K.R., 2008. The Berlin Brain–Computer Interface: accurate performance from first-session in BCI-naive subjects. IEEE Trans. Biomed. Eng. 55, 2452–2462.
Brodersen, K.H., Wiech, K., Lomakina, E.I., Lin, C.-s., Buhmann, J.M., Bingel, U., Ploner, M., Stephan, K.E., Tracey, I., 2012. Decoding the perception of pain from fMRI using multivariate pattern analysis. NeuroImage 63, 1162–1170.

Bromm, B., Treede, R.D., 1984. Nerve fibre discharges, cerebral potentials and sensations induced by CO_2 laser stimulation. Hum. Neurobiol. 3, 33–40.

Bromm, B., Treede, R.D., 1991. Laser-evoked cerebral potentials in the assessment of cutaneous pain sensitivity in normal subjects and patients. Rev. Neurol. (Paris) 147, 625–643.

Brooks, J., Tracey, I., 2005. REVIEW: from nociception to pain perception: imaging the spinal and supraspinal pathways. J. Anat. 207, 19–33.

Brown, J.E., Chatterjee, N., Younger, J., Mackey, S., 2011. Towards a physiology-based measure of pain: patterns of human brain activity distinguish painful from non-painful thermal stimulation. PLoS One 6, e24124.

Cooil, B., Rust, R.T., 1994. Reliability and expected loss: a unifying principle. Psychometrika 59, 203–216.

Cortes, C., Vapnik, V., 1995. Support-vector networks. Mach. Learn. 20, 273–297.

Cruccu, G., Gronseth, G., Alksne, J., Argoff, C., Brainin, M., Burchiel, K., Nurmikko, T., Zakrzewska, J.M., 2008. AAN-EFNS guidelines on trigeminal neuralgia management. Eur. J. Neurol. 15, 1013–1028.

Cruccu, G., Sommer, C., Anand, P., Attal, N., Baron, R., Garcia-Larrea, L., Haanpaa, M., Jensen, T.S., Serra, J., Treede, R.D., 2010. EFNS guidelines on neuropathic pain assessment: revised 2009. Eur. J. Neurol. 17, 1010–1018.

Davis, K.D., 2006. Recent advances and future prospects in neuroimaging of acute and chronic pain. Futur. Neurol. 1, 203–213.

Davis, K.D., 2011. Neuroimaging of pain: what does it tell us? Curr. Opin. Support. Palliat. Care 5, 116.

Davis, K., Moayedi, M., 2012. Central mechanisms of pain revealed through functional and structural MRI. J. Neuroimmune Pharmacol. 1–17.

Davis, K.D., Hutchison, W.D., Lozano, A.M., Tasker, R.R., Dostrovsky, J.O., 2000. Human anterior cingulate cortex neurons modulated by attention-demanding tasks. J. Neurophysiol. 83, 3575–3577.

Davis, K.D., Racine, E., Collett, B., 2012. Neuroethical issues related to the use of brain imaging: can we and should we use brain imaging as a biomarker to diagnose chronic pain? Pain 153, 1555–1559.

Delorme, A., Makeig, S., 2004. EEGLAB: an open source toolbox for analysis of single-trial EEG dynamics including independent component analysis. J. Neurosci. Methods 134, 9–21.

Downar, J., Crawley, A.P., Mikulis, D.J., Davis, K.D., 2000. A multimodal cortical network for the detection of changes in the sensory environment. Nat. Neurosci. 3, 277–283.

Downar, J., Mikulis, D.J., Davis, K.D., 2003. Neural correlates of the prolonged salience of painful stimulation. NeuroImage 20, 1540–1551.

Duda, R., Hart, P., Stork, D., 2000. Pattern Classification, Nonparametric Techniques. Wiley-Interscience Publication.

Gagliese, L., Melzack, R., 1997. Chronic pain in elderly people. Pain 70, 3–14.

Garcia-Larrea, L., Peyron, R., Laurent, B., Mauguiere, F., 1997. Association and dissociation between laser-evoked potentials and pain perception. Neuroreport 8, 3785–3789.

Garcia-Larrea, L., Frot, M., Valeriani, M., 2003. Brain generators of laser-evoked potentials: from dipoles to functional significance. Neurophysiol. Clin. 33, 279–292.

Haanpaa, M., Attal, N., Backonja, M., Baron, R., Bennett, M., Bouhassira, D., Cruccu, G., Hansson, P., Haythornthwaite, J.A., Iannetti, G.D., Jensen, T.S., Kauppila, T., Nurmikko, T.J., Rice, A.S., Rowbotham, M., Serra, J., Sommer, C., Smith, B.H., Treede, R.D., 2010. NeuPSIG guidelines on neuropathic pain assessment. Pain 152, 14–27.

Hu, L., Mouraux, A., Hu, Y., Iannetti, G.D., 2010. A novel approach for enhancing the signal-to-noise ratio and detecting automatically event-related potentials (ERPs) in single trials. NeuroImage 50, 99–111.

Hu, L., Liang, M., Mouraux, A., Wise, R.G., Hu, Y., Iannetti, G.D., 2011. Taking into account latency, amplitude, and morphology: improved estimation of single-trial ERPs by wavelet filtering and multiple linear regression. J. Neurophysiol. 106, 3216–3229.

Hüsing, B., Jäncke, L., Tag, B., 2006. Impact Assessment of Neuroimaging: Final Report.vdf Hochschulverlag AG.

Iannetti, G.D., Truini, A., Romaniello, A., Galeotti, F., Rizzo, C., Manfredi, M., Cruccu, G., 2003. Evidence of a specific spinal pathway for the sense of warmth in humans. J. Neurophysiol. 89, 562–570.

Iannetti, G.D., Zambreanu, L., Cruccu, G., Tracey, I., 2005. Operculoinsular cortex encodes pain intensity at the earliest stages of cortical processing as indicated by amplitude of laser-evoked potentials in humans. Neuroscience 131, 199–208.

Iannetti, G.D., Zambreanu, L., Tracey, I., 2006. Similar nociceptive afferents mediate psychophysical and electrophysiological responses to heat stimulation of glabrous and hairy skin in humans. J. Physiol. 577, 235–248.

Iannetti, G., Hughes, N.P., Lee, M.C., Mouraux, A., 2008. Determinants of laser-evoked EEG responses: pain perception or stimulus saliency? J. Neurophysiol. 100, 815–828.

Jung, T.P., Makeig, S., Westerfield, M., Townsend, J., Courchesne, E., Sejnowski, T.J., 2001. Analysis and visualization of single-trial event-related potentials. Hum. Brain Mapp. 14, 166–185.

Kakigi, R., Shibasaki, H., Ikeda, A., 1989. Pain-related somatosensory evoked potentials following CO_2 laser stimulation in man. Electroencephalogr. Clin. Neurophysiol. 74, 139–146.

Kenshalo, D.R., Iwata, K., Sholas, M., Thomas, D.A., 2000. Response properties and organization of nociceptive neurons in area 1 of monkey primary somatosensory cortex. J. Neurophysiol. 84, 719–729.

Koles, Z.J., 1991. The quantitative extraction and topographic mapping of the abnormal components in the clinical EEG. Electroencephalogr. Clin. Neurophysiol. 79, 440–447.

Koles, Z.J., Lazar, M.S., Zhou, S.Z., 1990. Spatial patterns underlying population differences in the background EEG. Brain Topogr. 2, 275–284.

Kunde, V., Treede, R.D., 1993. Topography of middle-latency somatosensory evoked potentials following painful laser stimuli and non-painful electrical stimuli. Electroencephalogr. Clin. Neurophysiol. 88, 280–289.

Lee, M.C., Mouraux, A., Iannetti, G.D., 2009. Characterizing the cortical activity through which pain emerges from nociception. J. Neurosci. 29, 7909–7916.

Legrain, V., Guerit, J.M., Bruyer, R., Plaghki, L., 2002. Attentional modulation of the nociceptive processing into the human brain: selective spatial attention, probability of stimulus occurrence, and target detection effects on laser evoked potentials. Pain 99, 21–39.

Legrain, V., Crombez, G., Verhoeven, K., Mouraux, A., 2011. The role of working memory in the attentional control of pain. Pain 152, 453–459.

Loeser, J.D., Treede, R.D., 2008. The Kyoto protocol of IASP basic pain terminology. Pain 137, 473–477.

Makeig, S., Jung, T.P., Bell, A.J., Ghahremani, D., Sejnowski, T.J., 1997. Blind separation of auditory event-related brain responses into independent components. Proc. Natl. Acad. Sci. U. S. A. 94, 10979–10984.

Marquand, A., Howard, M., Brammer, M., Chu, C., Coen, S., Mourão-Miranda, J., 2010. Quantitative prediction of subjective pain intensity from whole-brain fMRI data using Gaussian processes. NeuroImage 49, 2178–2189.

Mayhew, S.D., Iannetti, G.D., Woolrich, M.W., Wise, R.G., 2006. Automated single-trial measurement of amplitude and latency of laser-evoked potentials (LEPs) using multiple linear regression. Clin. Neurophysiol. 117, 1331–1344.

Mognon, A., Jovicich, J., Bruzzone, L., Buiatti, M., 2011. ADJUST: an automatic EEG artifact detector based on the joint use of spatial and temporal features. Psychophysiology 48, 229–240.

Mouraux, A., Iannetti, G.D., 2009. Nociceptive laser-evoked brain potentials do not reflect nociceptive-specific neural activity. J. Neurophysiol. 101, 3258–3269.

Mouraux, A., Diukova, A., Lee, M.C., Wise, R.G., Iannetti, G.D., 2011. A multisensory investigation of the functional significance of the "pain matrix". NeuroImage 54, 2237–2249.

Muller-Gerking, J., Pfurtscheller, G., Flyvbjerg, H., 1999. Designing optimal spatial filters for single-trial EEG classification in a movement task. Clin. Neurophysiol. 110, 787–798.

Ochsner, K.N., Ludlow, D.H., Knierim, K., Hanelin, J., Ramachandran, T., Glover, G.C., Mackey, S.C., 2006. Neural correlates of individual differences in pain-related fear and anxiety. Pain 120, 69–77.

O'Toole, A.J., Jiang, F., Abdi, H., Pénard, N., Dunlop, J.P., Parent, M.A., 2007. Theoretical, statistical, and practical perspectives on pattern-based classification approaches to the analysis of functional neuroimaging data. J. Cogn. Neurosci. 19, 1735–1752.

Prato, M., Favilla, S., Zanni, L., Porro, C.A., Baraldi, P., 2011. A regularization algorithm for decoding perceptual temporal profiles from fMRI data. NeuroImage 56, 258–267.

Raij, T.T., Numminen, J., Narvanen, S., Hiltunen, J., Hari, R., 2005. Brain correlates of subjective reality of physically and psychologically induced pain. Proc. Natl. Acad. Sci. U. S. A. 102, 2147–2151.

Ramoser, H., Muller-Gerking, J., Pfurtscheller, G., 2000. Optimal spatial filtering of single trial EEG during imagined hand movement. IEEE Trans. Rehabil. Eng. 8, 441–446.

Roulin, M.J., Ramelet, A.S., 2012. Pain indicators in brain-injured critical care adults: an integrative review. Aust. Crit. Care 25, 110–118.

Rust, R.T., Cooil, B., 1994. Reliability measures for qualitative data: theory and implications. J. Mark. Res. 31, 1–14.

Schnakers, C., Zasler, N.D., 2007. Pain assessment and management in disorders of consciousness. Curr. Opin. Neurol. 20, 620–626.

Schnakers, C., Chatelle, C., Majerus, S., Gosseries, O., De Val, M., Laureys, S., 2010. Assessment and detection of pain in noncommunicative severely brain-injured patients. Expert. Rev. Neurother. 10, 1725–1731.

Schulz, E., Zherdin, A., Tiemann, L., Plant, C., Ploner, M., 2012. Decoding an individual's sensitivity to pain from the multivariate analysis of EEG data. Cereb. Cortex 22, 1118–1123.

Seminowicz, D.A., Davis, K.D., 2006. Cortical responses to pain in healthy individuals depends on pain catastrophizing. Pain 120, 297–306.

Su, H., Du, P., Du, Q., 2012. Semi-supervised dimensionality reduction using orthogonal projection divergence-based clustering for hyperspectral imagery. Opt. Eng. 51, 111711–111718.

Tibshirani, R., 1996. Regression shrinkage and selection via the lasso. J. R. Stat. Soc.: Ser. B: Methodol. 267–288.

Tousignant-Laflamme, Y., Rainville, P., Marchand, S., 2005. Establishing a link between heart rate and pain in healthy subjects: a gender effect. J. Pain 6, 341–347.

Tracey, I., Mantyh, P.W., 2007. The cerebral signature for pain perception and its modulation. Neuron 55, 377–391.

Treede, R.D., Meyer, R.A., Raja, S.N., Campbell, J.N., 1995. Evidence for two different heat transduction mechanisms in nociceptive primary afferents innervating monkey skin. J. Physiol. 483 (Pt 3), 747–758.

Treede, R.D., Lorenz, J., Baumgartner, U., 2003. Clinical usefulness of laser-evoked potentials. Neurophysiol. Clin. 33, 303–314.

Valentini, E., Hu, L., Chakrabarti, B., Hu, Y., Aglioti, S.M., Iannetti, G.D., 2012. The primary somatosensory cortex largely contributes to the early part of the cortical response elicited by nociceptive stimuli. NeuroImage 59, 1571–1581.

Witten, I.H., Hall, M.A., 2011. Data mining: Practical Machine Learning Tools and Techniques3rd ed. Morgan Kaufmann, Amsterdam; London.

Zhang, H., 2004. The optimality of naive Bayes. AA1, 3.

Zhang, Z.G., Hu, L., Hung, Y.S., Mouraux, A., Iannetti, G.D., 2012. Gamma-band oscillations in the primary somatosensory cortex—a direct and obligatory correlate of subjective pain intensity. J. Neurosci. 32, 7429–7438.

Zwakhalen, S.M., Hamers, J.P., Abu-Saad, H.H., Berger, M.P., 2006. Pain in elderly people with severe dementia: a systematic review of behavioural pain assessment tools. BMC Geriatr. 6, 3.